THE JOURNAL OF PHYSICAL CHEMISTRY A

Article

pubs.acs.org/JPCA

Quasi-Classical Trajectory Study of Atom−Diatomic Molecule Collisions in Symmetric Hyperspherical Coordinates: The F + HCl Reaction as a Test Case

Victor Manuel Freixas-Lemus, Aliezer Martínez-Mesa,* and Llinersy Uranga-Piña

DynAMoS (Dynamical processes in Atomic and Molecular Systems), Facultad de Física, Universidad de la Habana, San Lázaro y L, La Habana 10400, Cuba

ABSTRACT: We investigate the reactive dynamics of the triatomic system F + HCl → HF + Cl for total angular momentum equal zero and for different low-lying rovibrational states of the diatomic molecule. For each of the initial vibrational quantum numbers, the time evolution of the atom−diatom collision process is investigated for a wide range of impact angles and collision energies. To this purpose, the Quasi-Classical Trajectories (QCT) method was implemented in a hyperspherical configuration space. The Hamilton equations of motion are solved numerically in an intermediate effective Cartesian space to exploit the relative simplicity of this intermediate representation. Interatomic interactions are described by a London−Eyring−Polanyi−Sato potential energy surface, specifically developed for the title reaction, and the results of the QCT simulations are discussed in terms of the time-evolution of the hyperangles. The analysis of the collision dynamics using symmetric hyperspherical coordinates provides, in addition to the description in terms of a natural reaction coordinate (the hyperradius), a more striking representation of the exchange dynamics, in terms of the time-dependent probability distribution along the kinematic rotation hyperangle, and a precise distinction between direct and indirect mechanisms of the reaction.

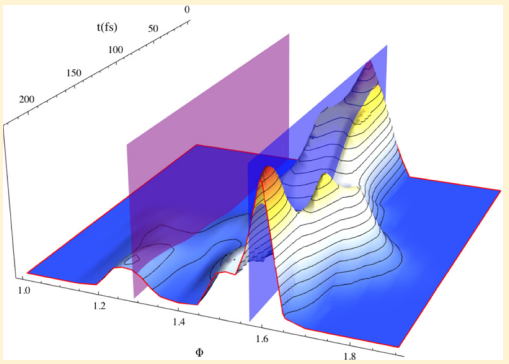

1. INTRODUCTION

Since its inception in the 1950s, molecular dynamics has evolved into a powerful and universal tool for the investigation of the atomic motion underlying time-dependent phenomena at the molecular scale. Progressively, new atomistic simulation techniques have been developed and successfully applied to the study of the dynamics of such systems. However, the computer power and memory requirements increase with the size of the system under study. Therefore, the size and complexity of molecular systems that can be simulated at present are limited by the current availability of computational resources. In spite of the pace of increase in computer performance, there will be also some limits in the future. As a consequence, there is a considerable interest in developing more efficient and simple representations of molecular motion.

A judicious choice of the coordinate system is usually of crucial importance for both the classical and the quantum treatments of the motion of several particles in space. Various alternative sets of coordinates (e.g., the Jacobi and the Radau-Smith vectors) have been employed in the description of the internal motion in three-body problems in general and for elementary chemical reactions particularly (see refs 1, 2, and refs therein). In this sense, hyperspherical coordinates have been successfully used for studying simple molecular systems, while they are very appealing for the theoretical description of polyatomic systems.[3−9] Likewise, they have been extensively applied in investigations in atomic[10,11] and nuclear[12,13] physics. Within the hyperspherical formalism, the motion of N particles in three-dimensional space is mapped into the motion of a single particle along the hyperradius and $3N - 3$ hyperangles, once the motion of the center of mass has been separated out. The hyperspherical coordinates are advantageous in the description of the asymptotic reaction channels[14] and chirality.[15−17]

In this paper we address the relationship between Smith−Whitten hyperspherical coordinates[18] and the instantaneous geometric distribution of three atoms (in their plane of motion) during three-particle exchange reactions. As a numerical application for triatomic systems, we investigate the time evolution of Smith−Whitten hyperspherical coordinates for the F + HCl reaction, with emphasis on the identification of the different channels based on these generalized coordinates (and especially on the so-called kinematic hyperangle). The target reaction has received a lot of attention in recent years.[19−27] This process belongs to the type heavy + light-heavy of atom−diatom collisions, which are of interest in the design of chemical lasers, due its low energy barrier, its exothermicity, and the high vibrational excitation of the HF product.[28]

We are interested in the understanding of the collision process at a microscopic, molecular level, that can be gained by examining the time evolution of the hyperspherical coordinates, rather than computing state-resolved reaction probabilities or

Received: November 25, 2015
Revised: March 17, 2016

DOI: 10.1021/acs.jpca.5b11525
J. Phys. Chem. A XXXX, XXX, XXX−XXX

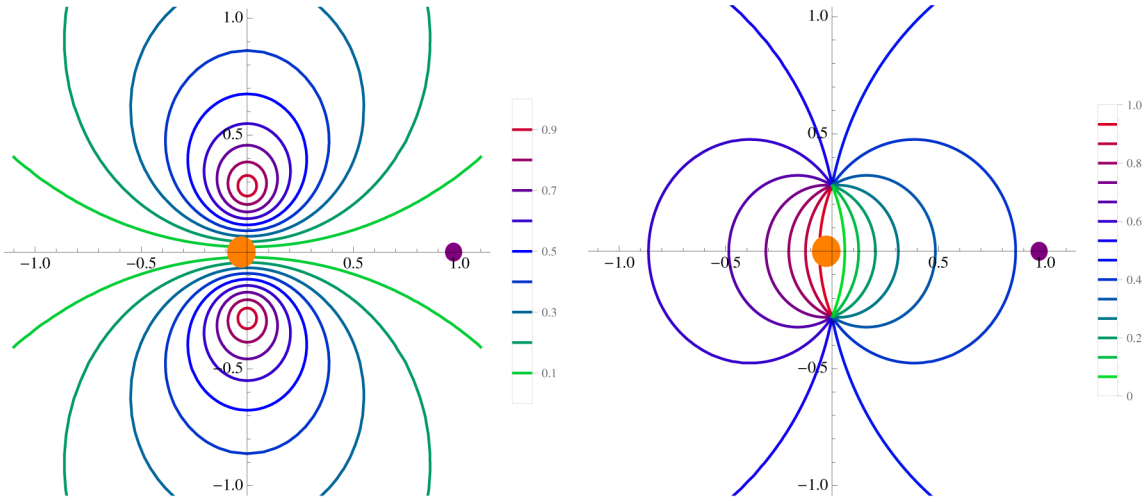

(a) Hyperangle $\Theta/(\pi/4)$. (b) Hyperangle Φ/π.

Figure 1. Variation of hyperangles Θ (expressed in units of $\pi/4$) and Φ (in units of π) as the position of F atom spans the plane of motion. The larger dot represents the Cl atom, while the smaller dot represents the H atom. The unit of length is the distance between Cl and H atoms.

rate constants. The detailed knowledge of the characteristics of the molecular motion in the hyperspherical configuration space may be used afterward in the design of new approximate methodologies for the theoretical modeling of the reaction dynamics in polyatomic systems. To this aim, the present study extends previous investigations on the hyperspherical representation of the potential energy function of triatomic systems[29−31] to the analysis of the time-dependent molecular dynamics. To our knowledge, studies of the time-dependent reaction dynamics in hyperspherical coordinates are scarce in the literature.[25,32−36] Most of the dynamical calculations employing the hyperspherical formalism focused on the analysis of reaction dynamics in the time-independent formulation.[9,37−46]

The paper is organized as follows. In Section 2, the Smith−Whitten hyperspherical coordinates are briefly introduced, and their properties relevant for the study of the three-particle reaction dynamics are described. In Section 3, the Hamiltonian and the equations of motion are presented, together with the main characteristics of the potential energy surface (PES) and the methodology employed in the quasi-classical trajectory calculations. In Section 4, the results concerning the representation of individual trajectories in the hyperspherical configuration space and the time evolution of the probability density distribution along the kinematic hyperangle are presented and discussed. Finally, the key aspects of the hyperspherical description of the time-dependent collision dynamics are summarized in Section 5.

2. SMITH−WHITTEN COORDINATES AND THE MAPPING OF THE GEOMETRICAL ARRANGEMENT OF THREE-PARTICLE SYSTEMS

For triatomic systems, the symmetric hyperspherical coordinates can be expressed as a function of the mass-scaled Jacobi vectors $\vec{r}$ and $\vec{R}$. In the present study, $\vec{r}$ is chosen as the vector from the Cl to the H atom, whereas $\vec{R}$ is set as the vector from F atom to the center of mass of the HCl diatomics.

After separating the motion of the center of mass of the triatomic system and the rigid body rotations of the system, the remaining degrees of freedom are the hyperradius

$$\rho = \sqrt{R^2 + r^2} \tag{1}$$

and the two hyperangles Θ and Φ, defined through the relations

$$\sin(2\Theta) = 2\frac{|\vec{R} \times \vec{r}|}{\rho^2} \tag{2}$$

$$\tan(2\Phi) = 2\frac{\vec{R}\cdot\vec{r}}{r^2 - R^2} \tag{3}$$

Among the many different possible parametrizations,[2] the set ρ, Θ, Φ, defined via the expressions (1)−(3), are considered "democratic" generalized coordinates, since they have no dependence on the particular choice of the ordering of the three atoms.

The hyperradius has a straightforward interpretation: it takes small values when the three particles are close to each other, and it becomes larger as the particles move apart. These properties single out the hyperradius as a natural reaction coordinate, parametrizing the collision involving the three particles.

One of the advantages of the hyperspherical formalism is the nearly adiabatic separation between the motion along the hyperradius and the hyperangular subspace. Such separation has been exploited to study the scattering dynamics by propagating along the hyperradius, using the eigenfunctions of the hyperangular Hamiltonian as a basis.[5,37,41,42,46,47] Moreover, some studies introduce a semiclassical integration scheme where the motion along the hyperradial coordinate is treated classically, while the Schrödinger equation was integrated numerically to update the dynamical state in the hyperangular subspace.[48]

To get a deeper insight into the physical meaning of hyperangles, we exploit their scale invariance, that is, the fact that the values of the hyperangles do not change if Jacobi vectors are increased (decreased) by the same factor, as long as the moduli of the Jacobi vectors remain different from zero. As an illustration of the connection between the point occupied by the system in the hyperspherical space and the geometrical

DOI: 10.1021/acs.jpca.5b11525
J. Phys. Chem. A XXXX, XXX, XXX−XXX

arrangement of the three particles, we show in Figure 1 the values of the hyperangles Θ and Φ for each position of the F atom, after fixing the positions of the Cl and the H atoms. These contour plots are independent of the distance between Cl and H atoms due to the aforementioned scale invariance.

The plots 1a,b become useful for understanding the time evolution of the hyperangles Θ and Φ during collisions between an atom and a diatomic molecule. For instance, Figure 1a shows that Θ vanishes if the three particles are aligned, which is helpful in detecting rotations of a diatomic molecule with respect to the third particle.

As we will show in the following, in this hyperspherical parametrization, the hyperangle Φ carries substantial information on the reaction branching among the different channels. If $\Phi < \pi/2$, then the F atom is placed in the right semiplane of Figure 1b; otherwise, the F atom is located in the left semiplane. This qualitative information aids to rationalize steric effects in terms of the direction in which the F atom approaches the HCl diatomic molecule.

Analyzing the time evolution of hyperangle Φ one can distinguish among the various reaction channels. In the reactant valley, corresponding to the stable configuration F + HCl, Φ takes the asymptotic value $\Phi_{HCl} = \pi/2$ (for an infinite separation between the F atom and the diatomic molecule). For the remaining stable configurations, Cl + HF and H + ClF, the hyperangle Φ takes the values Φ_{HF} and Φ_{ClF}, respectively. These limiting values are given by

$$\Phi_{HF} = \frac{1}{2}\arccos\left[\frac{(m_{Cl} + m_H)^2\mu_{HCl}^2 - m_{Cl}^2\mu^2}{(m_{Cl} + m_H)^2\mu_{HCl}^2 + m_{Cl}^2\mu^2}\right] \approx 0.41\pi \tag{4}$$

$$\Phi_{ClF} = \frac{1}{2}\arccos\left[\frac{(m_{Cl} + m_H)^2\mu - m_{Cl}m_H^2}{(m_{Cl} + m_H)^2\mu + m_{Cl}m_H^2}\right] \approx 0.97\pi \tag{5}$$

where m_{Cl}, m_F, and m_H are the masses of the Cl, F, and H atoms, and μ and μ_{HCl} are the reduced masses

$$\mu = \sqrt{\frac{m_{Cl}m_Hm_F}{m_{Cl} + m_H + m_F}} \tag{6}$$

of the three-particle system, and

$$\mu_{HCl} = \frac{m_{Cl}m_H}{m_{Cl} + m_H} \tag{7}$$

of the diatomics.

The hyperangle Φ constitutes a continuous generalization of the traditional concept of the skewing angle, introduced in the theory of reaction dynamics. During the dynamics, Φ varies continuously between the values corresponding to the configurations where the diatomic molecule of the system is infinitely far from the isolated atom.

3. METHODOLOGY

3.1. Hamiltonian and Equations of Motion. To simplify the propagation of the dynamical state of the system, the Hamiltonian and the equations of motion were written in a Cartesian space ξ, η, and ζ, first defined by Johnson:[49]

$$\xi = \rho\cos(2\Theta)\sin(2\Phi) \tag{8}$$

$$\eta = \rho\cos(2\Theta)\cos(2\Phi) \tag{9}$$

$$\zeta = \rho\sin(2\Theta) \tag{10}$$

For the case of total angular momentum equal zero, the resulting Hamiltonian reads:

$$H = \frac{1}{\mu}\left[4(P_\xi^2 + P_\eta^2 + P_\zeta^2) - 3\frac{(\xi P_\xi + \eta P_\eta + \zeta P_\eta)^2}{\xi^2 + \eta^2 + \zeta^2}\right] + V(\xi, \eta, \zeta) \tag{11}$$

where P_ξ, P_η, and P_ζ are the generalized momenta corresponding to ξ, η, and ζ, and V is the potential energy of the system. The equations of motion derived from this Hamiltonian are

$$\dot{s} = \frac{1}{\mu}[4P_s - 3Ws] \tag{12}$$

$$\dot{P}_s = \frac{3W}{\mu}[P_s - Ws] - \frac{\partial V}{\partial s} \tag{13}$$

where

$$W = \frac{\xi P_\xi + \eta P_\eta + \zeta P_\zeta}{\xi^2 + \eta^2 + \zeta^2} \tag{14}$$

and $s = \xi, \eta, \zeta$. The classical equations of motion were solved numerically in this effective Cartesian space, using the fourth-order Adams−Moulton method with a time step of $1 \times 10^{-2}\ \hbar/E_h$, started by a fourth-order Runge−Kutta integrator. Individual trajectories were propagated until one of the following criteria was met:

(i) the hyperradius became larger than $100a_0$, or
(ii) the total simulation time exceeded 4 ps.

For systems with total angular momentum J different from zero, rotational kinetic energy and Coriolis coupling terms can be expressed as functions of the symmetric hyperspherical coordinates.[49] However, the additional complexity of the Hamiltonian makes the extension of the present methodology for $J > 0$ a nontrivial task. Consequently, the results of the simulations presented in Section 4 are restricted to $J = 0$. Although the reaction dynamics can be different for nonzero J values, preliminary investigations on the validity of the proposed scheme (made on the basis of the comparison of state-to-state reaction probabilities and reaction rate constants, computed within the J-shifting approximation, with the corresponding experimental values) confirm the advantages of the hyperspherical formalism for the description of the quasi-classical reaction dynamics in triatomic systems for $J > 0$.

3.2. Potential Energy Surface. To expose the advantages of Smith−Whitten coordinate system as an interpretative tool for the exchange reaction dynamics, we performed several simulations of the collision process between a F atom and a HCl diatomic molecule. The interaction between the particles is represented by a London−Eyring−Polanyi−Sato (LEPS) PES.[50,51] The parameter values, which determine the shape of the LEPS PES, were taken from the literature.[19] This particular choice of the interaction potential was designed to optimize the correspondence between the results of Quasi-Classical Trajectory (QCT) calculations and the experimental data available for the F + HCl reaction. Because of the fitting of the experimental results, the possible role played by tunnelling (at low collision energies) or quantum delocalization effects are masked in the resulting potential landscape. Therefore, this PES represents a natural starting point for a QCT study of the time

DOI: 10.1021/acs.jpca.5b11525
J. Phys. Chem. A XXXX, XXX, XXX−XXX

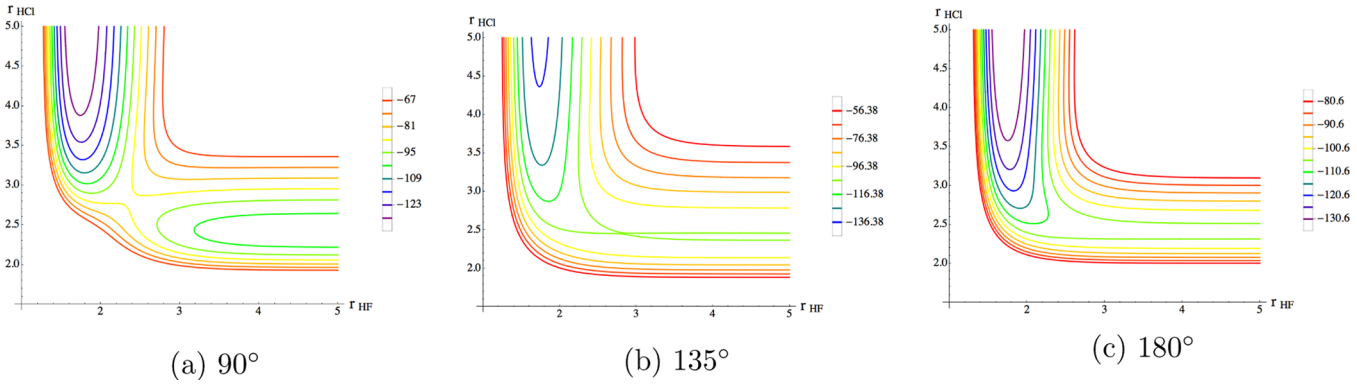

Figure 2. Contour plots of the potential energy of the triatomic system (in kcal·mol^{-1}), as a function of the interatomic distances HF and HCl, for various angles between the Jacobi vectors: (a) T-shape (90°), (b) 135°, and (c) collinear (180°) configurations.

evolution of the hyperangular variables during exchange reactions.

The contour plots in Figure 2 illustrate the angular dependence of the interaction potential. The potential energy profile does not exhibit any significant barrier along the reaction path. The reactant and product valleys are well-defined for T-shape configurations, whereas the latter gets broader (along the reaction coordinate) as the angle between Jacobi vectors varies from 90° to 180° (collinear geometry).

A deeper insight can be gained from the inspection of the PES represented as a function of the symmetric hyperspherical coordinates (Figure 3). The dashed line at $\Phi = \pi/2$ indicates

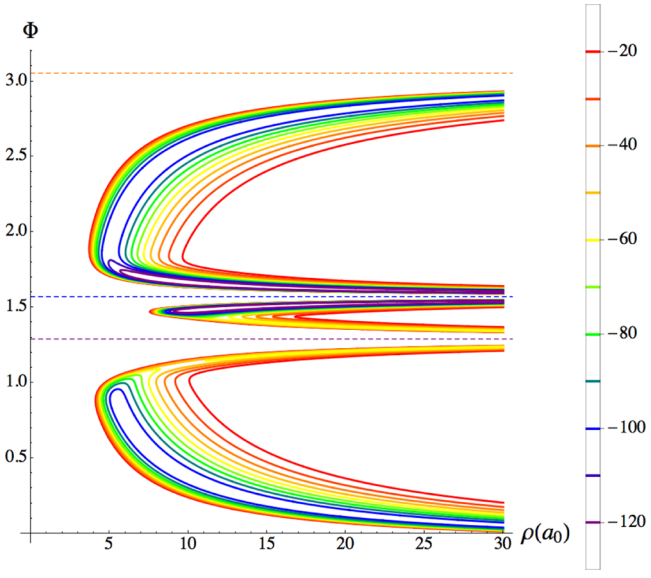

Figure 3. Contour plots of the LEPS PES (in kcal·mol^{-1}) as a function of the hyperspherical variables ρ (in atomic units) and Φ. The hyperangle Θ is set to zero, corresponding to an infinite atom−diatom separation.

the value of this hyperangle at the initial point in time ($\rho \to \infty$, $\Phi = \pi/2$). From this plot, it becomes striking that the two well-defined minima of the intermolecular potential along the coordinate Φ drive the splitting of the initial distribution in this direction, as the molecular density approaches the inner turning point (ρ_{min}). The reaction may proceed by moving forward along each well (approaching the asymptotic values Φ_{ClF} or Φ_{HF} of the hyperangle Φ) or by tracing back the incoming trajectory (in this case, $\Phi(t \to \infty) \to \Phi_{HCl}$).

3.3. Initial Conditions for the Quasi-Classical Trajectory Calculations. Initial conditions were generated in Jacobi coordinates by sampling the quantum-mechanical probability distributions in configuration and momentum spaces. The values of the HCl bond stretching coordinate r were generated to sample the probability density corresponding to the solution of the time-independent Schrödinger equation on the intramolecular potential. The latter is obtained as the limit of the LEPS PES when the F atom is infinitely far from the HCl diatomic molecule.

In Figure 4 we plotted the probability distribution corresponding to the low-lying vibrational states $|\Psi_0\rangle$, $|\Psi_1\rangle$, and $|\Psi_2\rangle$ of the HCl molecule. For these states, the probability density profiles closely follow those of the corresponding vibrational states $|\Upsilon_0\rangle$, $|\Upsilon_1\rangle$, and $|\Upsilon_2\rangle$ in the harmonic approximation. It can be noticed that the main difference consists in a relative displacement between the distributions. These spatial shifts do not modify the corresponding distributions in momentum space, which are nearly identical for the full potential and for the harmonic approximation. Therefore, the harmonic oscillator eigenfunctions in momentum space were used to sample initial conditions along P_r, while the exact vibrational eigenfunctions were used to sample the initial positions for the QCTs.

However, for every trajectory, the distance R between the center of mass of the HCl molecule and the F atom is generated using a Gaussian distribution centered at 10 Å with a standard deviation of 0.5 Å. Finally, for the impact angle, which is the initial angle between Jacobi vectors, we used a uniform distribution corresponding to the rotational ground state. Calculations are performed for different initial kinetic energies of the F atom (in the range from 0 to 150 kcal·mol^{-1}), and its velocity is chosen in the direction of the center of mass of the HCl molecule. For each collision energy, a swarm of 5000 trajectories sampling the aforementioned initial distributions was propagated according to the classical equations of motion. Observables such as the time-dependent probability density distribution along the kinematic hyperangle are calculated as histograms of this ensemble of nuclear trajectories.

In the hyperspherical picture, the initial probability density in both configuration and momentum spaces mimic the nodal structure of the vibrational wave function of the diatomic molecule. The projections of the momentum distributions in the $P_\rho P_\Theta$ plane, depicted in Figure 5, correspond to the

DOI: 10.1021/acs.jpca.5b11525
J. Phys. Chem. A XXXX, XXX, XXX−XXX

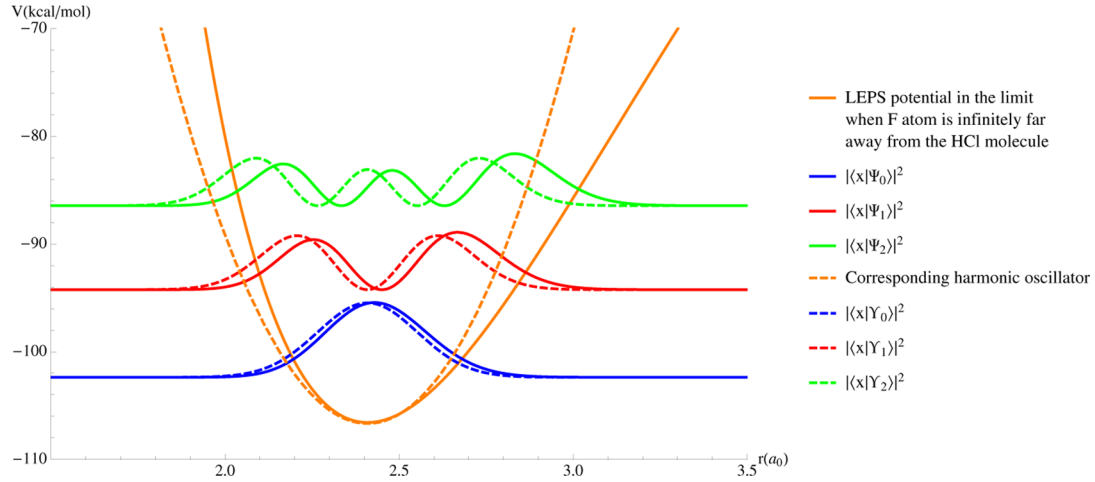

Figure 4. Potential energy curve along the HCl bond stretching coordinate (solid curve), obtained as the limit of the LEPS PES when the F atom is infinitely far from the diatomic molecule and its harmonic approximation (dashed curve). The probability densities corresponding to the ground, first excited, and second excited vibrational states on the LEPS potential (solid lines), and the corresponding harmonic oscillator solutions (dashed) are also shown.

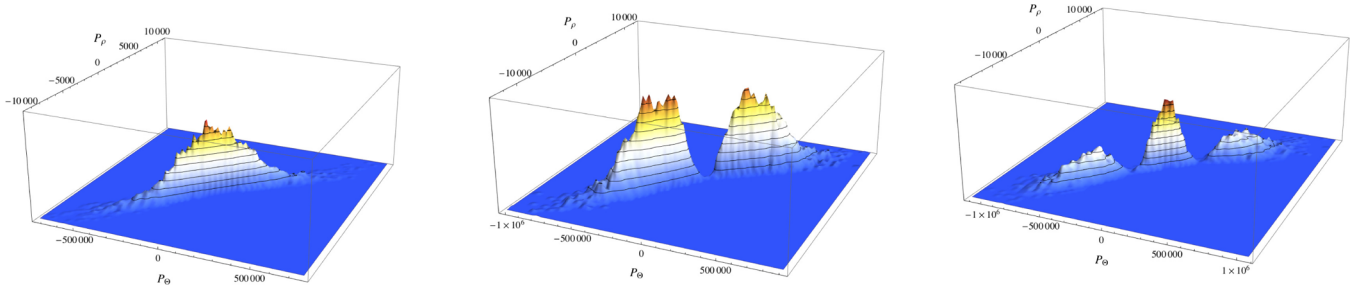

(a) Ground vibrational state (b) First excited state (c) Second excited state

Figure 5. Probability density in the hyperspherical momentum space, corresponding to the initial distribution of the QCTs for the vibrational (a) ground, (b) first, and (c) second excited states. The values of the conjugate momenta P_ρ and P_Θ are expressed in atomic units.

histograms of the initial conditions of the QCTs generated for each vibrational level of the molecule. They show that the conjugate momenta along the directions ρ and Θ are nearly proportional. Further, the vibrational excitation is reflected by the population of the regions in the hyperspherical phase space corresponding to higher momenta.

4. RESULTS

4.1. Quasi-Classical Trajectories in Hyperspherical Space. In this section, we will discuss the geometrical representation of characteristic trajectories, corresponding to the most important channels, in the hyperspherical configuration space.

In Figure 6 we show the time evolution of Smith−Whitten coordinates for an inelastic scattering trajectory. The fact that no exchange reaction is taking place can be inferred from the analysis of the asymptotic behavior of the hyperangle Φ at long times ($\Phi(t \to \infty) = \Phi(t \to 0) = \Phi_{HCl}$). It becomes apparent that the collision takes place at $t \approx 60$ fs, since the hyperradius attains its minimal value at this point of time. After the collision, the hyperangle Θ vanishes periodically, indicating the translational to vibrational energy transfer that causes the HCl molecule to rotate with respect to the position of F atom, in agreement with the trajectory displayed on the left panel. Finally, fingerprints of the intramolecular vibrations of the HCl diatomic molecule can be identified in the time evolution of both hyperangles.

While the trajectory represented in Figure 6 corresponds to a direct inelastic scattering, Figure 7 shows the time evolution of the symmetric hyperspherical coordinates for a typical indirect inelastic scattering. After the first collision, the F atom moves around the HCl diatomics for a relatively long time (in the picosecond time-scale). From the behavior of the hyperangle Θ, it becomes apparent that the intermediate complex formed by the three atoms lasts ∼15 rotational periods. After it orbits around the diatomic molecule during ∼1 ps, a second collision takes place, and the fluorine atom moves away from the hydrogen chloride.

A comparison between the frequencies of rotation during the collision and after it may shed some light on the nature of the energy redistribution process inside the intermediate triatomic complex. For instance, the rotation frequency of the HCl diatomic molecule during the intermediate phase is larger than its rotation frequency at longer times. From the energy conservation theorem, it follows that the F atom has less kinetic energy while orbiting around the HCl molecule than when it moves away from the vicinity of the diatom.

Figure 8 corresponds to another possible outcome of the collision: an exchange of the H atom, as it is indicated by the limiting value of the kinematic angle Φ. The time evolution of the hyperradius depicted in Figure 8 indicates that the collision

DOI: 10.1021/acs.jpca.5b11525
J. Phys. Chem. A XXXX, XXX, XXX−XXX

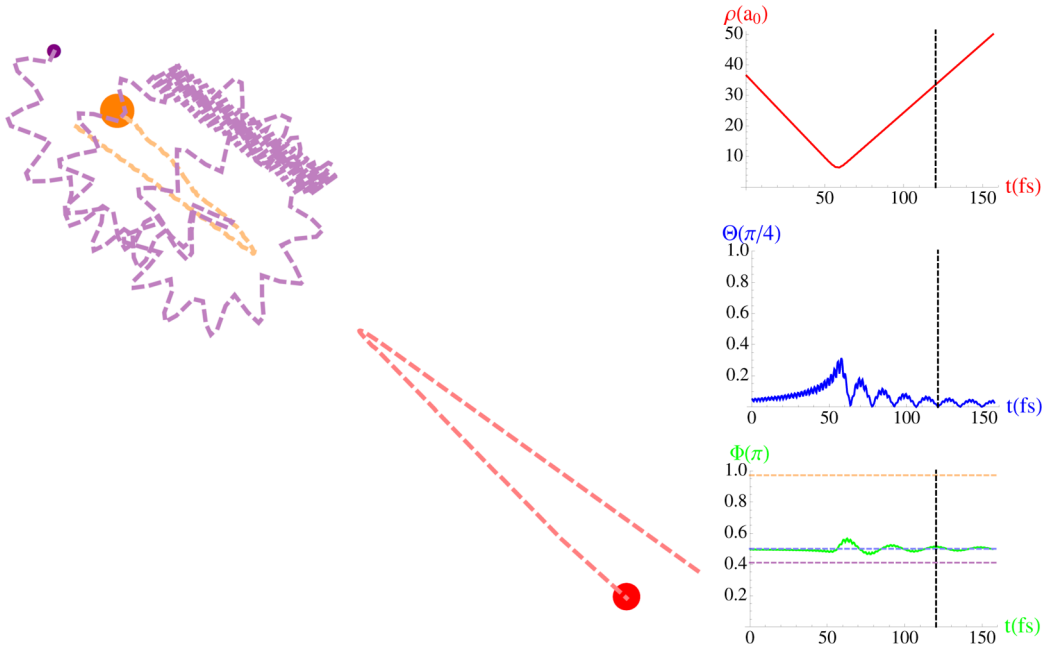

Figure 6. Time evolution of Smith−Whitten coordinates (right panels) for a representative inelastic scattering trajectory (displayed on the left), with a collision energy of 10 kcal·mol^{-1}. Initially, the HCl molecule is in the lowest vibrational state. The configuration displayed on the left correspond to the point in time marked by the vertical dashed line. The horizontal dashed lines in the undermost panel indicate the values corresponding to the stable configurations (from top to bottom, H + ClF, F + HCl, and Cl + HF). The hyperangles Θ and Φ are expressed in units of $\pi/4$ and π, respectively.

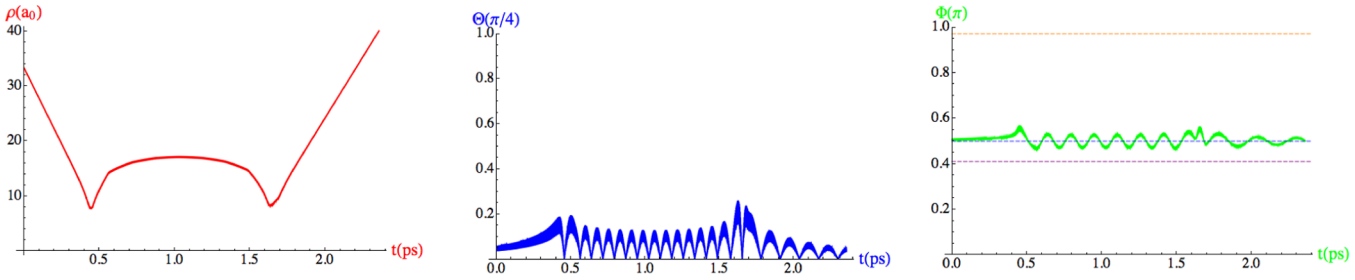

(a) Hyperradius ρ (b) Hyperangle Θ (c) Hyperangle Φ

Figure 7. Time evolution of Smith−Whitten coordinates for an inelastic scattering trajectory proceeding via the formation of an intermediate complex, with a collision energy of 0.1 kcal·mol^{-1}. The HCl molecule is initially in its second excited state. (c) The horizontal dashed lines indicate the values corresponding to the stable configurations (from top to bottom, H + ClF, F + HCl, and Cl + HF). The hyperangles Θ and Φ are expressed in units of $\pi/4$ and π, respectively.

takes place during a time interval of ∼30 fs, rather than being instantaneous as in the direct inelastic scattering analyzed previously (cf. Figure 6). In this case, the collision is followed by a backward scattering (i.e., it proceeds through the rebound reaction mechanism).[52] The process does not take place in a single step, but it consists of the following phases instead. First, a HF + Cl arrangement is adopted at t = 50 fs (as indicated by the instantaneous value of the kinematic hyperangle), and the reaction continues with the formation of a rotationally excited HCl molecule, before the H atom exchange takes place and the final HF product is formed. It can be noticed, that the F atom is initially placed in the right half plane of Figure 1b, and it remains in this region during the total time of the simulation.

Figure 9 depicts another possible reaction channel; that is, the time evolution of the hyperangle Φ indicates that the exchange of the Cl atom takes place during the reaction. Heavy-atom exchange is characterized by a larger variation of the position of the system in the hyperspherical configuration space, specifically along the coordinate Φ. However, the sudden change in the oscillation frequency of the hyperangle Θ indicates that the HCl bond breaks simultaneously with the formation of the ClF molecule (the marked reduction in the frequency of oscillation is associated with the larger reduced mass of the chlorine monofluoride, compared to the reactant diatomic molecule). The Cl-atom exchange also follows the rebound reaction mechanism. In this particular case, since the new molecule carries most of the mass of the system, oscillations can also be observed in the time evolution of the hyperradius. Finally, by inspecting the time evolution of the hyperangle Θ, we conclude that the vibrational excitation of the product molecule is not accompanied by rotations around the H atom, or at least the ClF diatom does not complete a 2π rotation during the total time of the simulation.

DOI: 10.1021/acs.jpca.5b11525
J. Phys. Chem. A XXXX, XXX, XXX−XXX

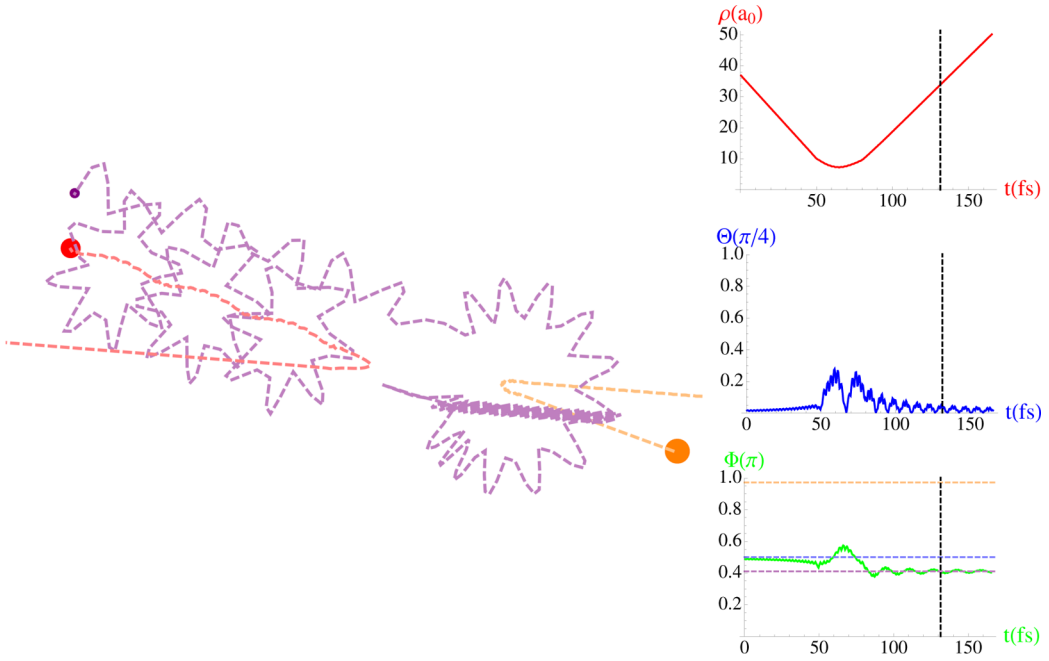

Figure 8. Time evolution of Smith−Whitten coordinates (right panels) for a representative H atom exchange trajectory (displayed on the left), corresponding to a collision energy of 10 kcal·mol^{-1}. The HCl molecule is initially in its second excited vibrational state. The configuration displayed on the left corresponds to the point in time marked by the vertical dashed line. The horizontal dashed lines in the undermost panel indicate the values corresponding to the stable configurations (from top to bottom, H + ClF, F + HCl, and Cl + HF). The hyperangles Θ and Φ are expressed in units of $\pi/4$ and π, respectively.

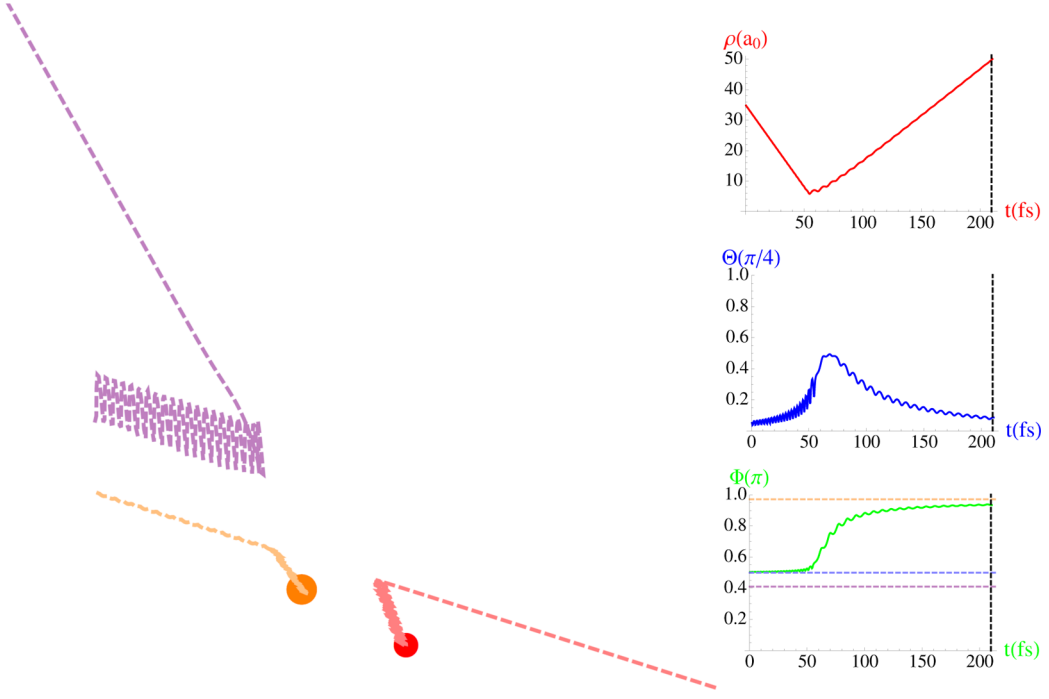

Figure 9. Time evolution of Smith−Whitten coordinates (right panels) for a representative Cl-atom exchange trajectory (represented on the left), with a collision energy of 10 kcal·mol^{-1}. The HCl molecule is initially in its second excited vibrational state. The configuration displayed on the left corresponds to the point in time marked by the vertical dashed line. The horizontal dashed lines in the undermost panel indicate the values corresponding to the stable configurations (from top to bottom, H + ClF, F + HCl, and Cl + HF). The hyperangles Θ and Φ are expressed in units of $\pi/4$ and π, respectively.

If the initial energy of the F atom is high enough, the triatomic system may undergo a different channel in which all particles move apart from each other. A typical collision-induced dissociation trajectory is displayed in Figure 10. This type of reaction may be easily distinguished from the others because, in general, the hyperangle Θ does not vanish as the hyperradius goes to infinity. Moreover, since molecular vibrations are no longer present after the collision event, no

DOI: 10.1021/acs.jpca.5b11525
J. Phys. Chem. A XXXX, XXX, XXX−XXX

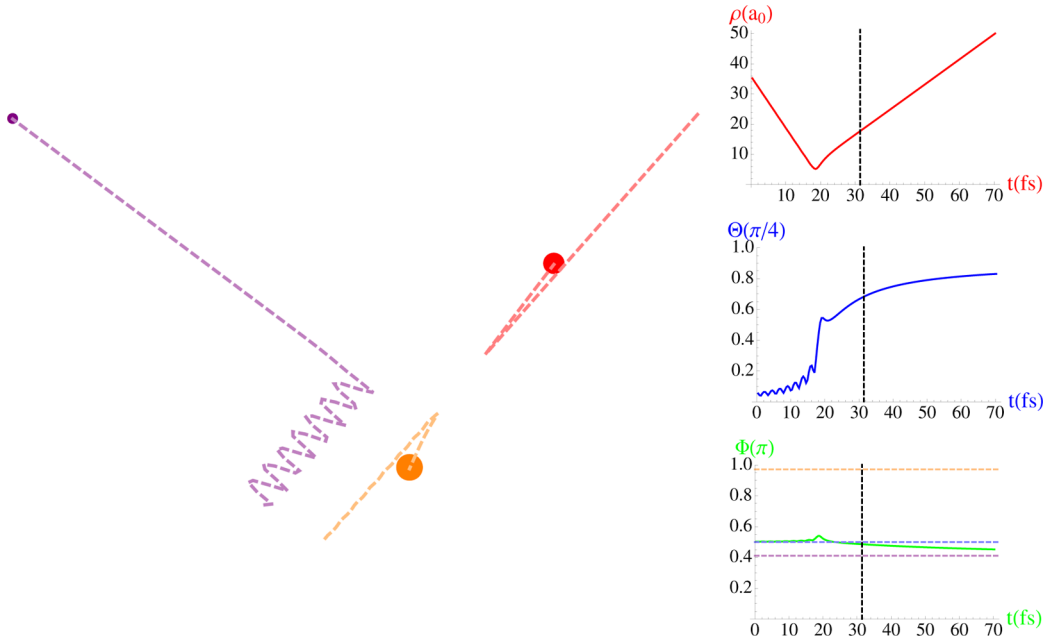

Figure 10. Time evolution of Smith–Whitten coordinates (right panels) for a typical collision-induced dissociation trajectory (represented on the left), with a collision energy of 100 kcal·mol^{-1}. The HCl molecule is initially in its first excited state. The horizontal dashed lines in the undermost panel indicate the values corresponding to the stable configurations (from top to bottom, H + ClF, F + HCl, and Cl + HF). The hyperangles Θ and Φ are expressed in units of $\pi/4$ and π, respectively.

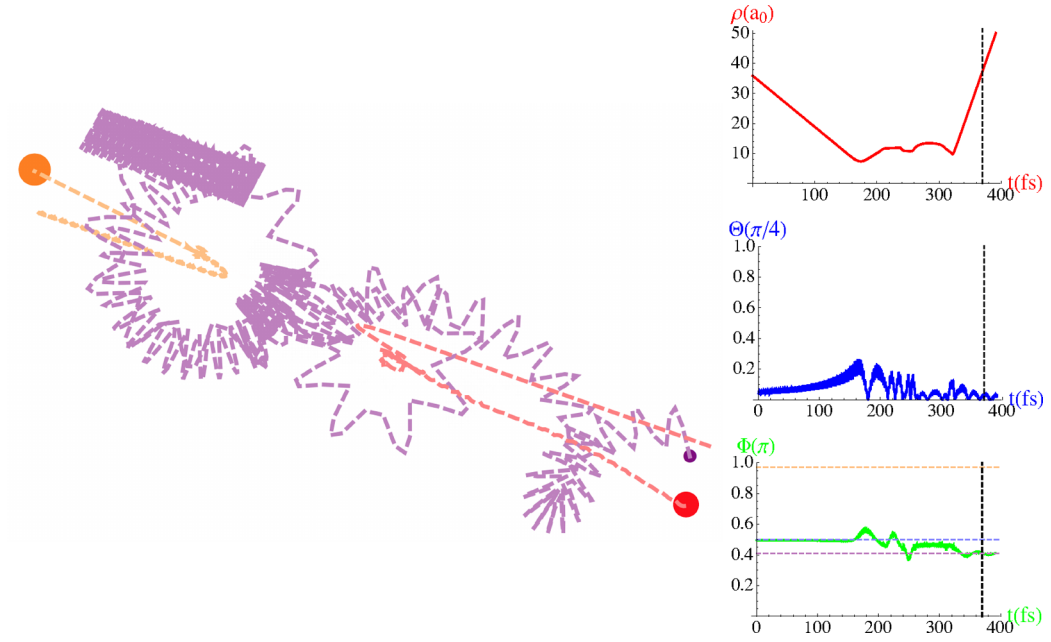

Figure 11. Time evolution of Smith–Whitten coordinates (right panels) for an inelastic scattering trajectory exhibiting a roaming behavior (displayed on the left), with a collision energy of 0.1 kcal·mol^{-1}. The HCl molecule is initially in its second excited vibrational state. The horizontal dashed lines in the undermost panel indicate the values corresponding to the stable configurations (from top to bottom, H + ClF, F + HCl, and Cl + HF). The hyperangles Θ and Φ are expressed in units of $\pi/4$ and π, respectively.

oscillatory patterns appear in the time evolution of any of the hyperangles. Finally, it can also be noticed that the hyperangle Φ does not evolve toward any of the asymptotic values corresponding to the (atom + diatom) stable configurations discussed above.

However, the trajectory displayed in Figure 11 does not correspond to a new channel, but it illustrates the occurrence of a peculiar kind of intermediate state. The reaction mechanism involves three collisions, before the system enters the product valley. After the first and the second encounters at t = 170 and 250 fs, the system exhibits configurations typical of an inelastic scattering trajectory (see the bottom panel in Figure 11). However, the resulting motion explores a different path, and it drives the system into the H atom exchange channel after the third collision takes place. This phenomenon has been termed as roaming, and it has attracted a lot of attention in recent years.[53,54] Roaming dynamics can be easily distinguished using Smith–Whitten coordinates, since the hyperradius remains

DOI: 10.1021/acs.jpca.5b11525
J. Phys. Chem. A XXXX, XXX, XXX–XXX

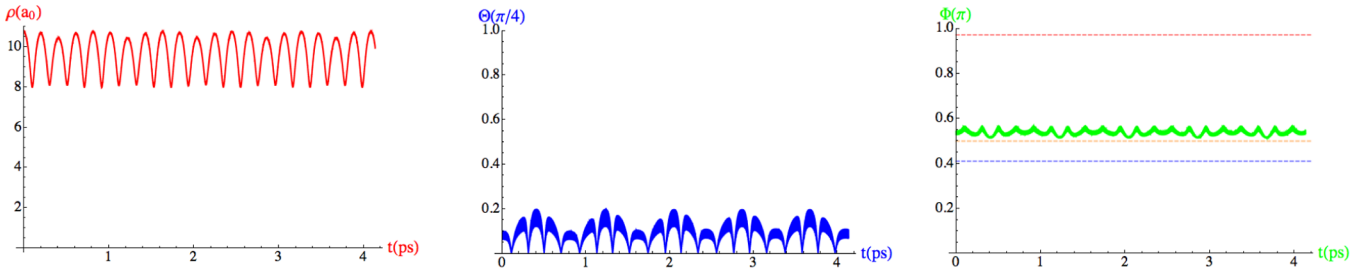

(a) Hyperradius ρ (b) Hyperangle Θ (c) Hyperangle Φ

Figure 12. Time evolution of Smith–Whitten coordinates for a triatomic compound. The horizontal dashed lines in the undermost panel indicate the values corresponding to the stable configurations (from top to bottom, H + ClF, F + HCl, and Cl + HF). The hyperangles Θ and Φ are expressed in units of $\pi/4$ and π, respectively.

approximately constant, while the triatomic system explores regions of the kinematic configuration space corresponding to several asymptotic stable configurations.

Finally, the behavior of a stable triatomic compound is investigated by artificially placing the F atom at a distance of 5 Å from the center of mass of the HCl molecule, with zero initial velocity. The resulting dynamics is shown in Figures 12a–c. The hyperradius undergoes bound oscillations indicating that the three particles remain close to each other. In contrast to the previous cases, the time evolution of the hyperangle Θ in Figure 12b reveals the presence of three, rather than two, oscillation frequencies. The three oscillation frequencies correspond to the three internal vibrational modes of the triatomic complex.

4.2. Time-Dependent Probability Density along the Kinematic Hyperangle. While a significant amount of information can be retrieved from the analysis of the time evolution of the hyperspherical variables along individual trajectories, the branching probabilities among the different channels are computed as statistical averages over a swarm of QCTs. In particular, the probability of hydrogen- or chlorine-atom exchange can be obtained from the integration of the density distribution along the coordinate Φ.

The time-evolution of the histogram of the hyperangles Φ, for trajectories starting with the HCl diatomics in its the ground vibrational state and with a collision energy of 10 kcal·mol^{-1}, is depicted in Figure 13. It can be observed that the potential energy maximum located at $\Phi = \pi/2$ (the maxima of the PES along this coordinate are indicated by the vertical planes in the upper panel) causes the early splitting of the molecular distribution. Each portion of density evolves subsequently in one of the adjacent potential wells (cf. Figure 3). During the first 130 fs, the density profile remains nearly symmetrical with respect to $\Phi = \pi/2$ as the two components of the distribution separate from each other, moving apart from the initial value Φ_{HCl}.

At t = 130 fs, the inner tail of the density profile reaches the maximum at Φ_{HF}, and this portion of the distribution subsequently crosses to the region $\Phi < \Phi_{HF}$. The fraction of the trajectories in the hemispace $\Phi < \pi/2$ evolves under the influence of the potential well in the neighborhood of Φ_{HF}. During the next 50 fs, it results in a rapidly oscillating density distribution, characterized by the presence of several small-amplitude ripples with varying positions and widths, which spreads over the kinematic hyperangular range around the Cl + HF and F + HCl configurations. After t = 180 fs, two well-defined maxima appear in the probability density in this region: the first one at $\Phi \lesssim \Phi_{HCl}$ and a notably less intense one

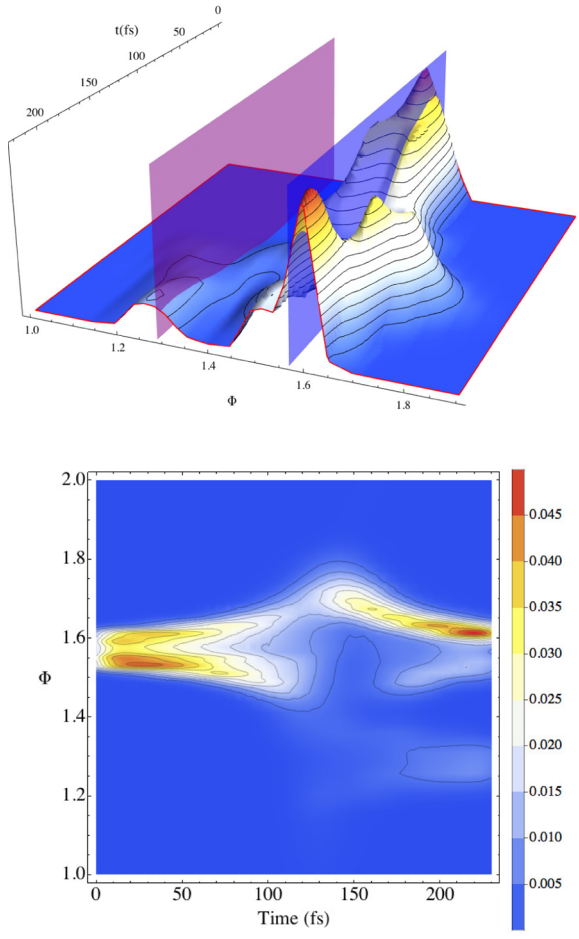

Figure 13. (a) Time evolution of the probability density along the hyperangle Φ. The vertical planes indicate the maxima of the LEPS PES in this direction, corresponding to the asymptotic stable configurations Cl + HF ($\Phi = 2\pi/5$) and F + HCl ($\Phi = \pi/2$). (b) Contour plots of the density distribution represented in the top panel.

centered at $\Phi \approx 2\pi/5$, indicating the formation of a HF molecule (the height of the former peak is twice as large as that of the latter). In the meantime, the direction of motion of the primary density peak gets reversed, and it approaches $\pi/2$ from above.

The final probability distribution shows that inelastic scattering is the dominant pathway (85.7% of the QCTs evolved into this channel), while the hydrogen exchange reaction has a markedly smaller probability of occurrence

DOI: 10.1021/acs.jpca.5b11525
J. Phys. Chem. A XXXX, XXX, XXX–XXX

(13.7%). However, the fraction of trajectories following the heavy-atom exchange channel is negligible (0.7%) for the range of collision energies investigated in this work.

5. CONCLUSIONS

We presented a QCT study of the collision process between a HCl diatomic molecule and an impinging F atom using Smith−Whitten hyperspherical coordinates, for total angular momentum equal zero. The hyperspherical formalism provides not only a flexible and efficient framework for the numerical integration of the equations of motion, but also a very appealing representation of the molecular dynamics wherein partitioning the hyperspherical configuration space results in a useful tool to discriminate the different channels or mechanisms.

The time dependence of the hyperspherical variables can be interpreted in terms of the modification of the molecular geometry along the reaction path. In particular, the time of occurrence and the duration of the molecular collision are directly indicated by the time-evolution of the hyperradius. However, collision-induced dissociation trajectories can be identified from the long-time behavior of the hyperangles:

1. the area-related variable Θ does not evolve to its linear configuration limit ($\Theta = 0$), and
2. the kinematic angle Φ does not approach any of the asymptotic values corresponding to the stable configurations.

The complete breakup of the triatomic complex is also characterized by the absence of oscillations in the time evolution of the hyperangles, indicating that there are no vibrating molecules in the system. Likewise, the remaining reaction channels can be identified from the long-time behavior of the hyperangle Φ.

The analysis of the time evolution of the hyperangles can be further exploited to extract more detailed information, such as from where the incident atom approaches the diatomics, or how the atoms rearrange during the collision event. The relationship between the rearrangement of the triatomic system during the course of the reaction, and the point occupied in the hyperspherical space, paves the way to the development of a geometrical intuition specific of the hyperspherical description. The latter may lead, for instance, to the development of new control strategies to steer chemical reactions in specific directions.

Furthermore, we performed a statistical analysis over swarms of QCTs representing specific initial states, from which the corresponding branching probabilities can be computed. In particular, the time-dependent yield of nondissociative channels is chiefly determined by the molecular distribution along the kinematic hyperangle Φ, and it can be calculated by integrating the projection of the density on this direction.

AUTHOR INFORMATION

Corresponding Author

*E-mail: aliezer@fisica.uh.cu. Phone: +53(0)78788956.

Notes

The authors declare no competing financial interest.

ACKNOWLEDGMENTS

This work was supported by the project PNCB-76-UH-15 of the Cuban National Program of Basic Sciences.

REFERENCES

(1) Hirschfelder, J. O. My Adventures in Theoretical Chemistry. *Annu. Rev. Phys. Chem.* **1983**, *34*, 1−30.
(2) Ragni, M.; Peixoto Bitencourt, A. C.; Aquilanti, V. *Hyperspherical and Related Types of Coordinates for the Dynamical Treatment of Three-Body Systems;* Lahmar, S. et al., Eds.; Topics in the Theory of Chemical and Physical Systems, Springer 2007; pp 123−146.
(3) Teplukhin, A.; Babikov, D. Interactive Tool for Visualization of Adiabatic Adjustment in APH Coordinates for Computational Studies of Vibrational Motion and Chemical Reactions. *Chem. Phys. Lett.* **2014**, *614*, 99−103.
(4) Teplukhin, A.; Babikov, D. Visualization of Potential Energy Function Using an Isoenergy Approach and 3D Prototyping. *J. Chem. Educ.* **2015**, *92*, 305−309.
(5) Lepetit, B.; Wang, D.; Kuppermann, A. Numerical Generation of Hyperspherical Harmonics for Tetra-Atomic Systems. *J. Chem. Phys.* **2006**, *125*, 133505−133513.
(6) Lombardi, A.; Palazzetti, F.; Peroncelli, L.; Grossi, G.; Aquilanti, V.; Sevryuk, M. B. Few-Body Quantum and Many-Body Classical Hyperspherical Approaches to Reactions and to Cluster Dynamics. *Theor. Chem. Acc.* **2007**, *117*, 709−721.
(7) Barreto, P. R. P.; Albernaz, A. F.; Palazzetti, F.; Lombardi, A.; Grossi, G.; Aquilanti, V. Hyperspherical Representation of Potential Energy Surfaces: Intermolecular Interactions in Tetra-Atomic and Penta-Atomic Systems. *Phys. Scr.* **2011**, *84*, 028111−028116.
(8) Riganelli, A.; Prudente, F. V.; Varandas, A. J. C. Evaluation of Vibrational Partition Functions for Polyatomic Systems: Quantum Versus Classical Methods for H_2O and Ar···CN. *Phys. Chem. Chem. Phys.* **2000**, *2*, 4121−4129.
(9) Aquilanti, V.; Cavalli, S.; De Fazio, D. Hyperquantization Algorithm. I. Theory for Triatomic Systems. *J. Chem. Phys.* **1998**, *109*, 3792−3804.
(10) Lin, C. D. Properties of High-Lying Doubly Excited States of H^-. *Phys. Rev. A: At., Mol., Opt. Phys.* **1982**, *25*, 1535−1545.
(11) Lin, C. D. Hyperspherical Coordinate Approach to Atomic and Other Coulombic Three-Body Systems. *Phys. Rep.* **1995**, *257*, 1−83.
(12) Delves, L. M. Tertiary and General-Order Collisions (II). *Nucl. Phys.* **1960**, *20*, 275−308.
(13) Simonov, Y. A. The Three Body Problem. A Complete System of Angular Functions. *Soviet J. Nucl. Phys.* **1966**, *3*, 461−466.
(14) Nakamura, H.; Ohsaki, A.; Baer, M. New Implementation to Approximate Quantum Mechanical Treatment of Atom-Diatom Chemical Reactions. *J. Phys. Chem.* **1986**, *90*, 6176−6184.
(15) Aquilanti, V.; Cavalli, S. The Quantum-Mechanical Hamiltonian for Tetraatomic Systems in Symmetric Hyperspherical Coordinates. *J. Chem. Soc., Faraday Trans.* **1997**, *93*, 801−809.
(16) Su, T.-M.; Palazzetti, F.; Lombardi, A.; Grossi, G.; Aquilanti, V. Molecular Alignment and Chirality in Gaseous Streams and Vortices. *Rend. Fis. Acc. Lincei* **2013**, *24*, 291−297.
(17) Palazzetti, F.; Tsai, P.-Y.; Lombardi, A.; Nakamura, M.; Che, D.-C.; Kasai, T.; Lin, K.-C.; Aquilanti, V. Aligned Molecules: Chirality Discrimination in Photodissociation and in Molecular Dynamics. *Rend. Fis. Acc. Lincei* **2013**, *24*, 299−308.
(18) Smith, F. T. A Symmetric Representation for Three-Body Problems. I. Motion in a Plane. *J. Math. Phys.* **1962**, *3*, 735−748.
(19) Kornweitz, H.; Persky, A. Quasiclassical Trajectory Calculations for the Reactions F + HCl, F + HBr, and F + HI. *J. Phys. Chem. A* **2004**, *108*, 140−145.
(20) Deskevich, M. P.; Hayes, M. Y.; Takahashi, K.; Skodje, R. T.; Nesbitt, D. J. Multireference Configuration Interaction Calculations for the F (^{2}P) + HCl → HF + Cl (^{2}P) Reaction: A Correlation Scaled Ground State (1^2A′) Potential Energy Surface. *J. Chem. Phys.* **2006**, *124*, 224303−224312.
(21) Hayes, M. Y.; Deskevich, M. P.; Nesbitt, D. J.; Takahashi, K.; Skodje, R. T. A Simple Picture for the Rotational Enhancement of the Rate for the F + HCl → HF + Cl Reaction: A Dynamical Study Using a New Ab Initio Potential Energy Surface. *J. Phys. Chem. A* **2006**, *110*, 436−444.

DOI: 10.1021/acs.jpca.5b11525
J. Phys. Chem. A XXXX, XXX, XXX−XXX

(22) Zolot, A. M.; Nesbitt, D. J. Quantum State Resolved Scattering Dynamics of F + HCl → HF (v,J) + Cl. *J. Chem. Phys.* **2007**, *127*, 114319−114331.
(23) Yin, S.; Guo, M.; Li, L.; Zhang, Y.; Li, X. Stereo-Dynamics of the F + HCl → HF + Cl Reaction. *Int. J. Quantum Chem.* **2011**, *111*, 4400−4409.
(24) Duan, Z. X.; Qiu, M. H.; Yao, C. X. Quasiclassical State-to-State Dynamics of the F + HCl Reaction on a Ground $1^2A'$ Potential Energy Surface. *Comput. Theor. Chem.* **2013**, *1024*, 69−75.
(25) Adhikari, S.; Varandas, A. J. C. The Coupled 3D Wave Packet Approach for Triatomic Reactive Scattering in Hyperspherical Coordinates. *Comput. Phys. Commun.* **2013**, *184*, 270−283.
(26) Li, A.; Guo, H.; Sun, Z.; Klos, J.; Alexander, M. H. State-to-State Quantum Dynamics of the F + HCl (v_i = 0, j_i = 0) → HF (v_f, j_f) + Cl Reaction on the Ground State Potential Energy Surface. *Phys. Chem. Chem. Phys.* **2013**, *15*, 15347−15355.
(27) Quéméner, G.; Balakrishnan, N. Cold and ultracold chemical reactions of F+HCl and F+DCl. *J. Chem. Phys.* **2008**, *128*, 224304−224304−11.
(28) Moore, C. M.; Smith, I. W. M.; Stewart, D. W. A. Rates of Processes Initiated by Pulsed Laser Production of F Atoms in the Presence of HCl, CH4, and CF_3H. *Int. J. Chem. Kinet.* **1994**, *26*, 813−825.
(29) Aquilanti, V.; Cavalli, S.; Grossi, G. Hyperspherical Coordinates for Molecular Dynamics by the Method of Trees and the Mapping of Potential Energy Surfaces for Triatomic Systems. *J. Chem. Phys.* **1986**, *85*, 1362−1375.
(30) Aquilanti, V.; Cavalli, S.; Grossi, G.; Anderson, R. W. Representation in Hyperspherical and Related Coordinates of the Potential-Energy Surface for Triatomic Reactions. *J. Chem. Soc., Faraday Trans.* **1990**, *86*, 1681−1687.
(31) Aquilanti, V.; Laganà, A. On the All Channels Representation of the Potential Energy Surface for Reactive Collisions. *Chem. Phys. Lett.* **1989**, *158*, 87−94.
(32) Marković, N.; Billing, G. D. The Coupled Three-Dimensional Wave Packet Approach to Reactive Scattering. *J. Chem. Phys.* **1994**, *100*, 1085−1093.
(33) Echave, J. Time-Dependent Reactive Scattering in Hyperspherical Coordinates: A Close Coupled Wave Packet Approach. *J. Chem. Phys.* **1996**, *104*, 1380−1386.
(34) Barinovs, G.; Marković, N.; Nyman, G. Split Operator Method in Hyperspherical Coordinates: Application to CH_2I_2 and OClO. *J. Chem. Phys.* **1999**, *111*, 6705−6711.
(35) Crawford, J.; Parker, G. A. State-to-State Three-Atom Time-Dependent Reactive Scattering in Hyperspherical Coordinates. *J. Chem. Phys.* **2013**, *138*, 054313−054325.
(36) Sahoo, T.; Ghosh, S.; Adhikari, S.; Sharma, R.; Varandas, A. J. C. Low-Temperature $D^+ + H_2$ Reaction: A Time-Dependent Coupled Wave-Packet Study in Hyperspherical Coordinates. *J. Chem. Phys.* **2015**, *142*, 024304−024313.
(37) Aquilanti, V.; Cavalli, S.; Volpi, A.; De Fazio, D. The A+BC Reaction by the Hyperquantization Algorithm: The Symmetric Hyperspherical Parametrization for J > 0. *Adv. Quantum Chem.* **2001**, *39*, 103−121.
(38) Parker, G. A.; Pack, R. T. Quantum Reactive Scattering in Three Dimensions Using Hyperspherical (APH) Coordinates. VI. Analytic Basis Method for Surface Functions. *J. Chem. Phys.* **1993**, *98*, 6883−6896.
(39) Babikov, D.; Kendrick, B. K.; Zhang, P.; Morokuma, K. Cyclic-N_3. II. Significant Geometric Phase Effects in the Vibrational Spectra. *J. Chem. Phys.* **2005**, *122*, 044315−044335.
(40) Quéméner, G.; Balakrishnan, N.; Kendrick, B. K. Quantum Dynamics of the O + OH → H + O_2 Reaction at Low Temperatures. *J. Chem. Phys.* **2008**, *129*, 224309−224316.
(41) De Fazio, D.; Aquilanti, V.; Cavalli, S.; Aguilar, A.; Lucas, J. M. Exact State-to-State Quantum Dynamics of the F + HD → F (v′ = 2) + D Reaction on Model Potential Energy Surfaces. *J. Chem. Phys.* **2008**, *129*, 064303−064311.
(42) Remmert, S. M.; Banks, S. T.; Clary, D. C. Reduced Dimensionality Quantum Dynamics of $CH_3 + CH_4$ → $CH_4 + CH_3$: Symmetric Hydrogen Exchange on an Ab Initio Potential. *J. Phys. Chem. A* **2009**, *113*, 4255−4264.
(43) Skouteris, D.; De Fazio, D.; Cavalli, S.; Aquilanti, V. Quantum Stereodynamics for the Two Product Channels of the F + HD Reaction from the Complete Scattering Matrix in the Stereodirected Representation. *J. Phys. Chem. A* **2009**, *113*, 14807−14812.
(44) Quéméner, G.; Kendrick, B. K.; Balakrishnan, N. Quantum Dynamics of the H + O_2 → O + OH Reaction. *J. Chem. Phys.* **2010**, *132*, 014302−014312.
(45) De Fazio, D.; de Castro-Vitores, M.; Aguado, A.; Aquilanti, V.; Cavalli, S. The He + H_2^+ → HeH^+ + H Reaction: Ab Initio Studies of the Potential Energy Surface, Benchmark Time-Independent Quantum Dynamics in an Extended Energy Range and Comparison with Experiments. *J. Chem. Phys.* **2012**, *137*, 244306−244320.
(46) De Fazio, D. The H + HeH^+ → He + H_2^+ Reaction from the Ultra-Cold Regime to the Three-Body Breakup: Exact Quantum Mechanical Integral Cross Sections and Rate Constants. *Phys. Chem. Chem. Phys.* **2014**, *16*, 11662−11672.
(47) Kuppermann, A. Quantum Reaction Dynamics and Hyperspherical Harmonics. *Isr. J. Chem.* **2003**, *43*, 229−241.
(48) Marković, N.; Billing, G. D. Semiclassical Wave Packet Approach to Reactive Scattering in Hyperspherical Coordinates. *J. Chem. Phys.* **1992**, *97*, 8201−8209.
(49) Johnson, B. R. The Classical Dynamics of Three Particles in Hyperspherical Coordinates. *J. Chem. Phys.* **1983**, *79*, 1906−1915.
(50) Polanyi, J. C. Infrared Chemiluminescence. *J. Quant. Spectrosc. Radiat. Transfer* **1963**, *3*, 471−496.
(51) Persky, A.; Klein, F. S. Kinetic Isotope Effects in the Reaction between Atomic Chlorine and Molecular Hydrogen. Tunnel Coefficients of the Hydrogen Atom through an Asymmetric Potential Barrier. *J. Chem. Phys.* **1966**, *44*, 3617−3626.
(52) *Theory of Chemical Reaction Dynamics;* Laganà, A.; Lendvay, G., Eds.; Springer, 2004.
(53) Mauguière, F. A. L.; Collins, P.; Ezra, G. S.; Farantos, S. C.; Wiggins, S. Roaming Dynamics in Ketene Isomerization. *Theor. Chem. Acc.* **2014**, *133*, 1−13.
(54) Joalland, B.; Shi, Y.; Kamasah, A.; Suits, A. G.; Mebel, A. M. Roaming Dynamics in Radical Addition-Elimination Reactions. *Nat. Commun.* **2014**, *5*, 1−6.

DOI: 10.1021/acs.jpca.5b11525
J. Phys. Chem. A XXXX, XXX, XXX−XXX